PROCEEDINGS, Twenty-Third Workshop on Geothermal Reservoir Engineering
Stnnford University, Stanford, California, January 26-28, 1998
SGP-TR-158

COMPARATIVE STUDY OF FRACTURES IN CORE AND BOREHOLE TELEVIEWER IN WELL VC-2B, VALLES CALDERA, NEW MEXICO

Dennis L. Nielson', Colleen A. Barton[2] and Kelly E. Keighley[1]

1. Energy & Geoscience Institute, University of Utah
423 Wakara Way
Salt Lake City, Utah 84108
dnielson@egi.utah.edu
2. Department of Geophysics, Stanford University
BS7 Mitchell Building
Stanford, California 94305
barton@pangea.stanford.edu

ABSTRACT

Well VC-2B is a continuous core hole drilled in the Sulphur Springs area of the Valles caldera, New Mexico. It reached a temperature of 295° C at a total depth of 5780 feet. Borehole televiewer logs are available for the depth interval of 704 feet to 910 feet where measured temperatures are about 140" to 145" C. This interval is the principal zone of lost circulation in the well and contains numerous fractures that can be identified as faults, mode I extensional fractures, hydrothermal breccias and completely and partially sealed fractures. The zones responsible for the lost circulation can be identified in the core by the presence of drilling mud, lost circulation material and migrated fines derived from both the rock and drill string. Analysis of fractures from the televiewer log of VC-2B shows that most of them strike to the northeast and dip steeply to the northwest, parallel to the Sulphur Creek fault zone.

INTRODUCTION

There is a very poor understanding of the character of fractures that host high-temperature fluid production. Existing models are adapted from outcrop studies that typify faults as containing a core zone where most of the strain is accommodated, surrounded by a damage zone that hosts a network of subsidiary fractures (Forster et al., 1997). Experience suggests that it is the fault cores that provide the exceptional permeability required for economic production of geothermal fluids, and the damage zone largely contributes to reservoir storage (Nielson, 1997). However, there are few examples that are well documented by core or image logs to use in the evaluation of this statement.

Efforts to map fractures in the subsurface remain a problem in geothermal exploration and development. Borehole imaging is an extremely useful technique for orienting fractures intersected by a geothermal well. Imaging logs are generally of two types: borehole televiewer **(BHTV)** that provides an acoustic image and tools that generate electrical resistivity images of the borehole wall. This study uses the televiewer that is described in Glowka et al. (1990). Recently, a great deal of imaging has been done in the Dixie Valley geothermal system (Barton et al., 1997), research that is still in progress.

GEOLOGIC SETTING

The Valles caldera is one of the largest and youngest silicic magmatic centers in North America (Smith et al., 1970; Heiken et al., 1990). Eruptions of the Otowi (1.45 Ma) and Tschirege (1.12 Ma) members of the Bandelier Tuff each had volumes estimated at 300 km^3, and each formed thick sections of densely welded ash flow tuff within the caldera (Nielson and Hulen, 1984).

The Valles caldera was the site of a major geothermal exploration effort that investigated two areas: the Redondo dome where most of the wells were drilled, and the Sulphur Springs area that saw more limited commercial exploration (Dondanville, 1978). The Sulphur Springs area was the location for drilling two continuous core holes under the Continental Scientific Drilling Program, VC-2A and VC-2B, that were drilled in the vicinity of old geothermal exploration wells (Fig. 1). VC-2B was the deeper and **hot**ter, reaching a depth of 5780 feet and a temperature of 295" C (Hulen et al., 1989). A lithologic log of the core is presented in Hulen and Gardner (1989).

Several lines of evidence suggest that the Sulphur Springs area has undergone a complex hydrothermal history (Hulen and Nielson, 1986, 1988; Goff and Gardner, 1994). Alteration mineralogy and fluid inclusion data both show that temperatures were higher in the past and were subsequently lowered, perhaps through the draining of a caldera lake. This essentially instantaneous reduction in pressure was probably responsible for hydrothermal brecciation and flooding of fractures by clay minerals.

The Valles caldera is located at the intersections of the northeast trending Jemez Lineament and the NS trending Rio Grande Rift. Faults showing both of these regional trends are present within the caldera. In addition, there are fractures that result from caldera formation, in particular, ring fractures and those that were probably formed during resurgent doming. Thus, this is classified as a composite structural system utilizing both inherited regional structural grains and fractures formed during caldera development. VC-2B is located to the east of the Sulphur Creek fault (SCF) as shown in Fig. 1. Electrical resistivity surveying across this structure suggests that it has an offset of 400 to 500 m but was not intersected by VC-2B (Wannamaker, 1997). **As** mapped to the north of VC-2B, the SCF has a strike of N35°W to N42°W (Fig. 1). The Freelove Canyon fault has a strike of about N50°W and is probably inherited from the Jemez Lineament.

DRILLING AND LOGGING

VC-2B was drilled to total depth using a wireline coring system. Of particular interest for this study are the drilling operations that took place through the interval we are studying. The driller's log indicates the hole was initially cored and then reamed to 9-5/8 inch diameter to a depth of 707 feet. Then, 6-5/8 inch casing was set to a depth of 700 feet. On the televiewer log, the bottom of the casing is located at 703.9 feet. The hole was then cored using CHD-134 rods to a depth of 2092 feet. Beneath the casing, the driller's log shows that circulation was lost at a depth of 870 feet, and that circulation was "all gone" at a depth of 890 feet. During the next drilling shift, the crew began running mica in the hole to cure the lost circulation. The success of this was gauged by the hole being able to hold fluid at a depth of 350 feet. Casing was cemented in the hole to a depth of 1959 feet prior to the continuation of coring using CHD-IO1 rods. Thus, the interval we are studying was affected by drilling activities for some period of time after the core was originally collected. **A** logging program that

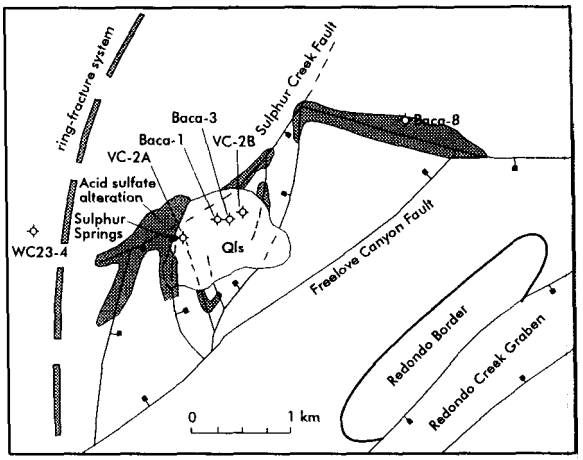

Fig. 1. Generalized geology of the Sulphur Spring: area showing well locations (Goff and Gardener, 1994).

Temperature Log Analysis

Several temperature logging runs were completed in the VC-2B corehole, and selected logs are shown in Fig. 2. Importantly, the temperature data was recorded at 1/2-foot intervals yielding excellent detail. Zones of lost fluid circulation are demonstrated by

Figure 3a shows the RDO11-6 temperature log with a plot of the calculated gradient that gives a better definition to the fluid loss zones. From this data, we have determined that the fluid was principally lost in the following zones that are defined by gradients of 0: 748.5 to 754 feet, 778.5 to 787 feet, 819 to 840.5 feet and 865 to 914.5 feet.

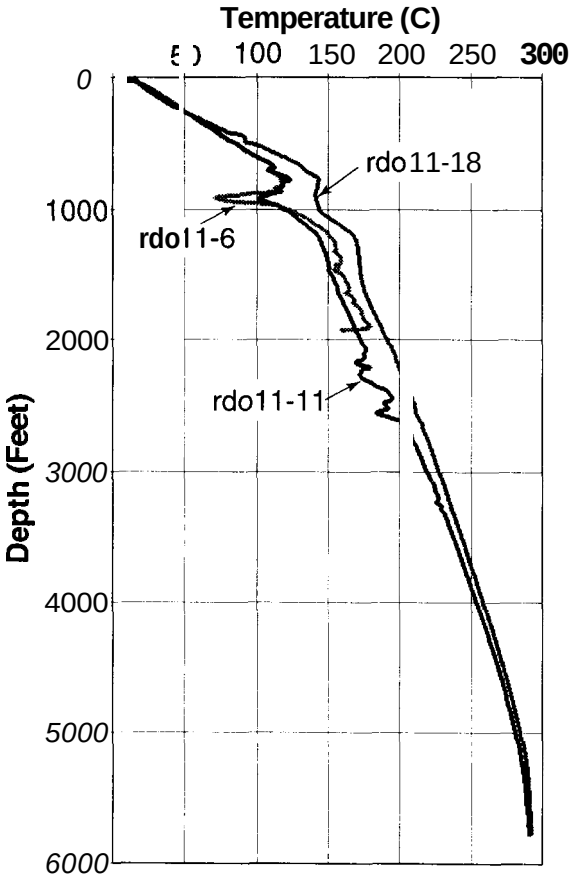

Fig. 2. Temperature logs for VC-2B. See text for profile identification.

Televiewer Log Analysis

Approximately 211 feet of open-hole BHTV data were recorded in the VC-2B drillhole in August 1988 following completion of the hole to 2092 feet. Digitization of the standard analog BHTV data results in the dual measurement of the acoustic reflectivity of the borehole wall and the ultrasonic travel time of the imaging pulse (see Zemanek et al., 1972 for a description of the BHTV tool operation). Post-logging digital data acquisition requires analog to digital conversion which was completed at the Stanford University Borehole Imaging Laboratory.

A software package designed for the analysis of digital BHTV data was used to process the digital data for noise and off-center tool effects. A five-point median filter was used to mitigate noise from spurious voltage surges and beam scattering in the data recorded in the wells. The image data requires calibration for borehole diameter prior to analysis. The calibration information used in this study was a nominal bit diameter of 13.4 cm. Using this information, recorded travel time data are converted to borehole radius values. The wellbore image data were corrected for magnetic declination directly after conversion from raw data format to the format of the image analysis software.

Fractures provide permeable pathways for fluids and further affect rock properties by facilitating chemical alteration of the surrounding rock mass. The relative importance of fractures in controlling rock properties depends on the fracture density and orientation as well as on the hydraulic and mechanical characteristics of the fractures themselves. The borehole televiewer provides excellent data for both detecting fractures with apertures larger than about 0.5 cm and for determining lithologic changes with depth.

One of the main uses of BHTV data is the measurement of the orientation and distribution of planar features in a drillhole. Planar features that intersect the borehole appear as sinusoids on unwrapped 360° views of the image data (Fig. 4). These sinusoids are often discontinuous for fine-scale fractures and they can show very complex patterns at points where several fractures intersect or where fractures are not perfectly planar.

The digital analysis of planar features is accomplished interactively using GMI•Imager™ with a 2-D image of the data over the fracture interval and a fracture measurement tool, a flexible sinusoid that is fit to the trace of fracture plane in the image. Once the feature is selected, the software records the depth, orientation, and apparent aperture. We use the term apparent aperture because the width of a fracture can be mechanically enlarged at its intersection with the drillhole by the drilling process. This means that fracture aperture as preserved in the BHTV log is an upper bound to the true aperture of the fracture at some distance away from the borehole. Sets of steeply dipping fractures were intersected in the study well. Many of these features appear as subvertical cracks in the image data. A specialized graphical measurement tool is used to determine the azimuth and dip of these subvertical fractures.

Measurement of apparent fracture aperture requires prior measurement of the orientation of the fracture plane to correct for the true structural dip of the fracture. With the amplitude and phase of the sinusoid determined, the wire frame "core" image can be rotated into the plane of the fracture and the fracture width can be interactively measured on the rotated image (Barton et al., 1991). Once the fracture orientation

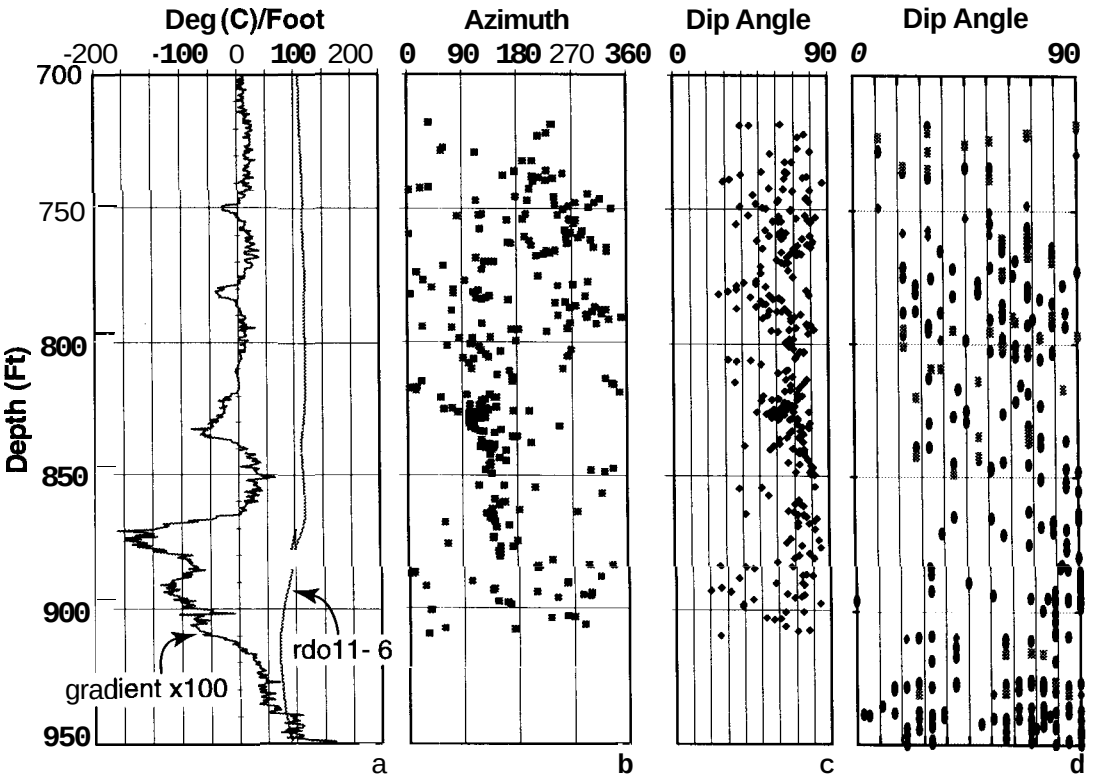

Fig. 3. Depth plots for interval studied in VC-2B a) Temperature log and calculated gradient, b) Dip azimuth and c) Dip angle plots from BHTV interpretation, and d) Dip angle of fractures measured on core. Solid dots are undifferentiated fractures, squares are faults and diamonds are mode I fractures.

and the apparent aperture have been measured, the measurement is available for further data reduction. The data recorded are depth, dip direction, dip, aperture, and feature classification (e.g., natural fracture, fault zone, bedding, etc.).

Fracture orientation was systematically measured using the processing system summarized above. The orientations of fractures measured in well VC-2B are plotted as a function of depth in Fig. 3b and c. Detailed interactive analysis of borehole televiewer data reveals a dominant northeast striking, steeply dipping fracture population for the VC-2B well. The fracture population for well VC-2B is dominated by high-angle fractures, and a histogram of the number of fractures per foot shows that the fracture distribution is not significantly changed as a function of depth. Although these results are from a somewhat shallower depth interval than other published data on the depth dependence of fracture frequency, they are similar to a number of other studies (Seeburger and Zoback, 1982; Barton and Zoback, 1989) which show no decrease in fracturing with depth.

Where fractures are open along the borehole, apparent fracture aperture could be measured. A fracture aperture profile was constructed by calculating the percentage of apparent apertures measured with the BHTV for each one-foot interval in the well. Intervals with a high frequency of fractures generally correspond to a high cumulative width per foot in the drillhole. Where the apparent aperture per foot is large, there are usually a larger number of fractures.

Core Analysis

A geologic log has been published for the core from the VC-2B hole (Hulen and Gardner, 1989), and the interested reader is directed to that publication for more detailed lithologic descriptions. The entire interval being studied is within partially to densely welded tuffs of the Tschirege Member of the Bandelier Tuff. Core samples are often incomplete because of loss of material during the drilling process, sampling by previous researchers, and mechanical damage during transport. Our analysis of the core was directed toward several objectives. First, we identified the origin of the fractures observed in the core and evaluated the application of fault zone models discussed above. Second, we estimated the qualitative permeability of fractures in the core by identifying the lost circulation material (LCM) that has

invaded the rock and correlation with the temperature logs. Third, we compared features seen in the core with those observed in the televiewer log.

Fractures form by a number of different mechanisms, and, in active geothermal systems, they are constantly modified by hydrothermal processes. In many cases in VC-2B, the mode of formation can be identified. In general, fracture displacement may be perpendicular to the fracture surface (termed dilational fractures, joints or mode I) or shear displacements parallel to the fracture surface, termed mode II (in-plane shear, normal fault) or mode III (anti-plane shear, strike-slip fault) fractures (Atkinson, 1987; Pollard and Aydin, 1988).

Faults in VC-2B have been identified by the presence of slickenlines along the fault plane. Unfortunately, the welded ash flow tuffs in VC-2B are not distinctive enough to visually determine offset of lithologic units. In a number of instances, we have not been able to determine origin and have used the term fracture. The identified faults are principally steep with slickenlines that demonstrate normal movement. Many are apparently permeable as shown by the presence of drilling mud and LCM.

Characterization of fractures included: a) the depth and relative trace length of fracture intersecting core; b) the type of fracture (e.g. fault, mode I, fracture with or without alteration, breccia, and/or vein); c) a qualitative estimate of permeability of the fracture using the presence of LCM, drilling mud, and/or mica; d) an identification and description of alteration minerals, fillings, and coatings associated with a particular fracture; e) the core texture near fractures; and f) an aperture measurement, where available.

Zone I, from 748.5 to 754 ft, is the smallest zone of lost circulation studied (Fig. 4). The minimum fracture intensity, compensating for the potential for missing or damaged core, is 2.47 fractures/ft in this zone. Faults, mode I, and fractures of unknown origin are present within this interval. Four faults were identified and are predominatly steeply dipping (70°-85°), with one fault having a shallow dip (20"). Well developed slickenlines, crystalline and amorphous quartz, white sericite, pyrite, minor calcite, and rare rhodochrosite (Hulen and Gardner, 1989) mark the fault surfaces. Also, a dark gray sulfide-rich silicification marks the fault surface and penetrates less than 0.13 cm of the core. Fault apertures and/or alteration halos surrounding the fault surface average between 0.13 to 1 cm. The trace lengths of the fault planes intersecting the core are aipproximately 0.1 to 1.4 ft, and increase the vertical connectivity by linking other fracture sets in this zone. Open segments of fault surfaces in the core are coated with drilling mud and a few contain LCM, suggesting these fractures constitute a permeable zone.

At least four mode I fractures occur within Zone I. The mode I fractures are manifested by the curved appearance of the crack tip and lack of offset. Because of the curvilinear nature of the fractures, the dip along one fracture surface varies with average dips between 70" to 90". These fractures are typically tight and appear partially to fully healed with measured apertures from 0.06 to 0.13 cm. However, in some cases the fractures are open and are coated with minor amounts of drilling mud and LCM, indicating slight permeability.

The next major zone of lost circulation, Zone 11, is located in the depth interval of 778.5 to 787 ft (Fig. 3a). Physical evidence for increased porosity within the core, including dissolution (etched) textures, brecciation, and vugs, markedly increases at a depth of 775.5 ft. Between 780 to 787 ft, a rubble fault zone exists with abundant open spaces, etching, and fillings of euhedral quartz crystals. This intensely fractured, etched, and brecciated zone extends to 791 ft in the core. The fracture intensity for Zone II is 1.06 fractures/ft; however, this is a minimum approximation since the core is severely broken and impossible to piece back together. Based on physical characteristics, most of the fractures inventoried in this zone are mode I and fractures of unknown origin. The presence of faulting is suggested by alteration along fracture surfaces which has been associated elsewhere in the core with faulting. Nonetheless, the relative displacement is uncertain so the fracture origin is undetermined. The fractures are shallow to steeply dipping, ranging from 20" to 85°. Two major breccia zones, at 780.42 ft and 789.5 ft, dip approximately 70" and are 2.5 to 5 cm thick. Numerous fractures terminate and/or extend from these breccia zones. Abundant LCM is found throughout the etched, brecciated, and vuggy openings within the core. Minor amounts of LCM are observed on a few of the fracture surfaces.

Zone III is located between about 819 and 840.5 ft. (Fig. 3a). This correlates well with an intensely fractured, etched, and brecciated region from roughly 819 to 843 ft on the core; and also includes a hydrothermal breccia dike with a 70" dip from 817 to 819.5 ft. A breccia up to 3 cm thick at 832.65 ft is also observed

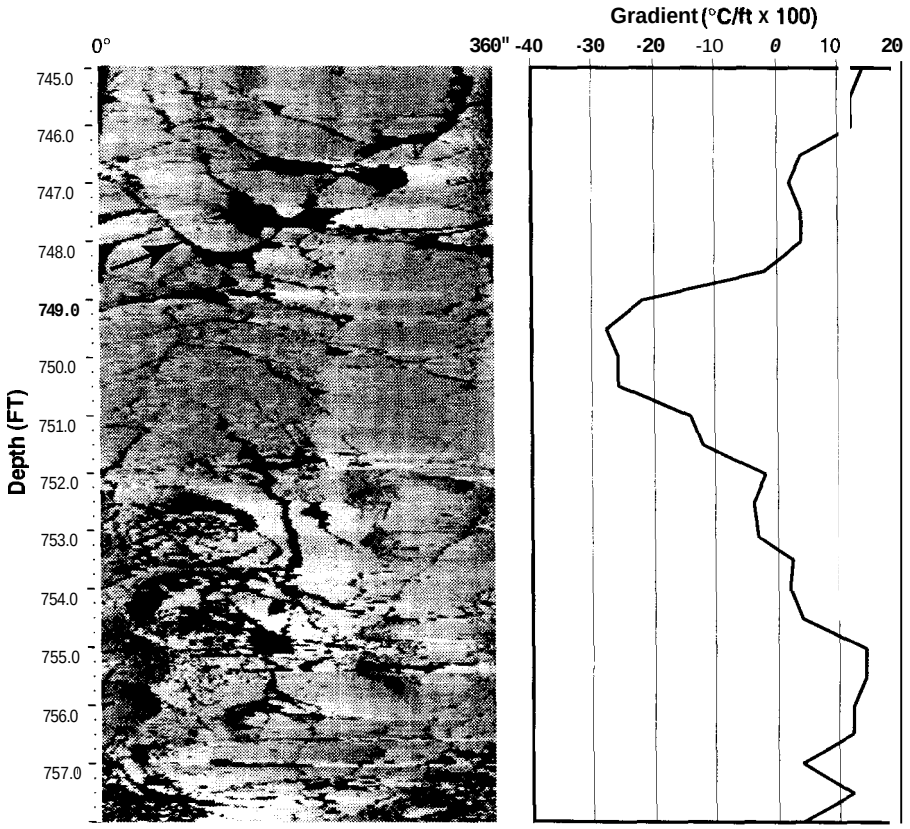

Fig. 4. BHTV image and temperature gradient of Zone I. Arrow shows sinusoidal form of fracture.

in this zone of the core and is of probable fault origin. Continuous and highly connective fractures exist from 825.9 to 834 ft, and 838 to 840 ft. The remaining portions of this zone are dominated by etched, vuggy. and brecciated textures with numerous small fractures connected to these features. The minimum fracture intensity for this zone is 2.8 fractures/foot. Fracture apertures range from 0.2 cm to 1.5 cm, with 0.6 cm the most common and the larger aperture values associated with vugs and/or etched fracture zones. Fractures are shallow to steeply dipping, with 60" to 75" dips common. Five faults, with average dips between 40" to 90°, are present within this zone, Drilling mud and LCM are found on a few fracture surfaces and within the etched, brecciated, and vuggy zones. The permeability of fractures may be increased if they are connected to faulted, etched, brecciated, or vuggy regions.

Zone IV is the most significant lost circulation zone and corresponds to a depth interval of 865 to 914.5 ft on the temperature log. The minimum fracture intensity for this zone is approximately 1.5 fractures/ft. On the core, an intensely fractured area which takes generous amounts of LCM begins at 857.5 ft, slightly shallower than the temperature log picks. From **863** to 870 ft there is a transition to a predominatly etched, brecciated, intensely fractured (dips range between *55"* to 90°), and healed region that takes abundant LCM . **A** steeply dipping (80") silicified fault-related breccia up to 5 cm thick occurs at 868 ft. From 870 to 875.3 ft there are several large, continuous fractures, possibly faults. Large continuous fractures, with or without alteration, and only trace amounts of LCM are the primary feature at a depth of 875.3 to 880.6 ft. From 880.6 to 884 ft, large continuous fractures and veins up to 1.3 cm thick are filled with quartz, pyrite, and coated with LCM. An intensely fractured, etched, and brecciated region occurs from 884 to 914 ft. Breccia zones within this interval average 1.3 cm thick. The fractures in this interval have a high connectivity and persistence, and plentiful LCM.

COMPARISON OF LOGS AND CORE

The BHTV for Zone I demonstrates an increase in fracture intensity within the depth intervals from 745 to 750.5 ft and 751 to 755.5 ft (Fig. 4). Measurements from the core are in good agreement with the televiewer analysis and show an increase in fracture intensity from 745.8 to 750.95 and 752.1 to 755 ft. The televiewer analysis identifies the frac-

tures, whereas the core analysis provides further physical evidence for the presence of several faults within this zone. The fracture intensity determined from televiewer data is 2.32 frac/ft. This correlates well with the fracture intensity observed in the core for this zone (2.47 frac/ft).

The BHTV and core correspond extremely well in Zone 11. Fractures observed on the image around 775.5 ft enlarge and become more connected from 778.5 to 789.5 ft. Similar features are observed in the core, with an etched and vuggy zone extending from 776 to 780 ft, a fault zone developing at 780 ft, and an increase in the degree of fracturing to a depth of 791 ft. The fracture intensity for the televiewer log is 2.13 frac/ft, while the fracture intensity of core is only 1.06 frac/ft. However, through this zone the core is incomplete and the fracture intensity is underestimated.

The BHTV displays an intensely fractured, etched, and brecciated zone, presumably Zone III, at approximately 817 to 847 ft. The temperature logs indicate a lost circulation zone slightly smaller than this, from 819 to 840.5 ft. A persistent zone of fractured, etched, and brecciated core exists from a depth interval of 819 to 843 ft. Etched and brecciated regions of the core occur both above and below this depth interval on the core; however, the fracture connectivity is much less. The fracture intensities are similar, with a televiewer fracture intensity of 2.02 frac/ft and a core fracture intensity of 2.8 frac/ft.

Zone IV, exhibits an increasingly fractured, brecciated, and etched zone from 859 to 910 ft. Note that the televiewer image log ends at 910 ft. The core shows an alternating zone of either predominantly fractured and faulted or brecciated and etched regions from a depth interval of 857.5 to 914 ft. Comparison of the fracture intensities of the logs is favorable and is 1.12 frac/ft for the televiewer log and 1.5 frac/ft for the core.

Figure 3b and c shows the orientation of fractures interpreted from the televiewer log. The Azimuth vs Depth plot shows a concentration of the fractures with a dip azimuth of 130° (N40°E strike). This is the orientation of the SCF and also the principal zone of fluid loss between 865 and 914.5 feet. Considering also the temperature and lithologic data, we would propose that the drill has intersected a normal fault zone parallel to the SCF. Our interpretation is that the principal zone of fluid loss represents the principal displacement zone (PDZ or core zone in the terminology of Forster et al, 1997) of the fault. The hanging wall contains the damage zone and extends as high as 748 feet. **As** shown in the core, this zone contains a variety of features including faults, breccias, and mode I fractures; however, it has more limited permeability than the PDZ.

In general, the distribution of the fractures in the core and the dip angles measured are comparable between the core and the BHTV, although more vertical dips were measured from the core than in the log interpretation. There is a suggestion that fluid loss identified in the core by the presence of LCM is often associated with faulting.

CONCLUSIONS

At this point, the core and temperature and televiewer logs should be considered to be complementary data sets. The core provides the best option for the identification of the origin of fractures while the BHTV provides information on their orientation. The detailed temperature logs are required to understand the permeability of the intersected fracture zones. We are not able to distinguish faults from other fractures on the BHTV, but this may be a function of both the resolution of the tool and the homogeneity of the lithologic section.

ACKNOWLEDGMENTS

This research was supported by the U. **S.** Department of Energy under contract DE-AC07-95ID 13274. Allan Sattler of Sandia was instrumental in securing the televiewer logs, providing funding for their interpretation, and encouraging our efforts We appreciate receiving the temperature data from Ron Jacobson also from Sandia National Laboratory.

REFERENCES

Atkinson, B. K., 1987, Introduction to fracture mechanics and its geophysical application, in Atkinson, B. K. (ed) Fracture Mechanics of Rocks: Academic Press, New York, p.1-26.

Barton, C.A., Hickman, **S.,** Morin, R., Zoback, M. D., Finkbeiner, T., Sass, J. and Benoit, D., 1997, Fracture permeability and its relationship to in situ stress in the Dixie Valley, Nevada, geothermal reservoir: Proceedings, 22nd Workshop on Geothermal Reservoir Engineering, Stanford University, p. 147-152.

Barton, C. A., Tesler, L. and Zoback, M. D., 1991, Interactive analysis of borehole televiewer data, in Palaz, I. and S. Sengupta (eds) Automated Pattern Analysis in Petroleum Exploration: Springer Verlag, New York, p. 223 - 248.

Barton, C. A. and Zoback, M.D., 1992, Self similar distribution and properties of macroscopic fractures at depth in crystalline rock in the Cajon Pass scientific drillhole, Journal Geophysical Research, v. 97, p. 518 1-5200.

Dondanville, R. F., 1978, Geologic characteristics of the Valles caldera geothermal system, New Mexico: Geothermal Resources Council Transactions, v. 2, p. 157-160.

Forster, C. B., Caine, J. S., Schultz, S. and Nielson, D. L., 1997, Fault zone architecture and fluid flow: an example from Dixie Valley, Nevada: Proceedings, 22nd Workshop on Geothermal Reservoir Engineering, Stanford University, p. 123-130.

Glowka, D. A., Loeppke, G. E., Lysne, P. C. and Wright, E. K., 1990, Evaluation of a potential borehole televiewer technique for characterizing lost circulation zones: Geothermal Resources Council Transactions, v 14, p. 395-402.

Goff, F. and Gardner, J. N., 1980, Geologic map of the Sulphur Springs geothermal system, Valles caldera, New Mexico: Los Alamos Scientific Laboratory Map, LA-8634-MAP.

Goff, F. and Gardner, J. N., 1994, Evolution of a mineralized geothermal system, Valles caldera, New Mexico: Economic Geology, v. 89, p. 1803-1832.

Goff, F., Gardner, J. N., Solbau, R. D., Adams, A., Evans, W. C., Lippert, D. R., Jacobsen, R., Bayhurst, G., Trujillo, P. E., Counce, D. and Dixon, P., 1990, The "art" of *in situ* fluid sampling and the remarkable compositional variations in the wellbore fluid of VC-2B, Valles caldera, New Mexico: Geothermal Resources Council Transactions, v. 14, p. 403-410.

Heiken, G., Goff, F., Gardner, J. N., Hulen, J. B., Nielson, D. L. and Vaniman, D., 1990, The Valles/Toledo caldera complex, Jemez volcanic field, New Mexico: Annual Reviews of Earth and Planetary Science, v. 18, p. 27-53.

Hulen, J. B. and Gardner, J. N., 1989, Field geologic log for Continental Scientific Drilling Program corehole VC-2B Valles caldera, New Mexico: University of Utah Research Institute report ESL-89025-TR, 92 p.

Hulen, J. B. and Nielson, D. L., 1986, Stratigraphy and hydrothermal alteration in well Baca-8, Sulphur Springs area, Valles caldera, New Mexico: Geothermal Resources Council Transactions, v. 10, p. 187-192.

Hulen, J. B. and Nielson, D. L., 1988, Clay mineralogy and zoning in CSDP corehole VC-2A: further evidence for collapse of isotherms in the Valles caldera: Geothermal Resources Council Transactions, v. 12, p. 291-298.

Hulen, J. B., Gardner, J. N., Goff, F., Nielson, D. L., Moore, J. N., Musgrave, J. A., Lemieux, M. M., Meeker, K. and Snow, M. G., 1989, The Sulphur Springs hydrothermal system, past and present: initial results from Continental Scientific Drilling Program corehole VC-2B, Valles caldera, New Mexico: Geothermal Resources Council Transactions, v. 13, p. 149-156.

Nielson, D. L., 1997, Rock permeability in high- temperature geothermal systems: Proceedings, Intersociety Energy Conversion Engineering Conference, Honolulu, p. 1837-1839.

Nielson, D. L. and Hulen, J. B., 1984, Internal geology and evolution of the Redondo dome, Valles caldera, New Mexico: Journal of Geophysical Research, v. 89, p. 8695-8711.

Pollard, D. D. and Aydin, A., 1988, Progress in understanding joining over the past century: Geological Society of America Bulletin, v. 100, p. 1181-1204.

Seeburger, D. A. and Zoback, M. D., 1982, The distribution of natural fractures and joints at depth in crystalline rock, Journal Geophysical Research, v. 87, p. 5517-5534.

Smith, R. L., Bailey, R. A. and Ross, C. S., 1970, Geologic map of the Jemez mountains, New Mexico: U. S. Geological Survey Miscellaneous Geologic Investigations Map 1-571.

Wannamaker, P. E., 1997, Tensor CSAMT survey over the Sulphur Springs thermal area, Valles caldera, New Mexico, U.S.A., Part I: Implications for structure of the western caldera: Geophysics, v. 62, p. 451-465.

Zemanek, J., Glenn, E. E., Norton, L. J. and Caldwell, R. L., 1970, Formation evaluation by inspection with the borehole televiewer: Geophysics, v. 35, p. 254-269.